BOULDER TRACKS WITHIN FINSEN CRATER: EVALUATION OF TRIGGERS.

T. Ruj[1], G. Komatsu[2], K. Kawai[1], H. Okuda[1,3], Z. Xiao[4], and D. Dhingra[5]. [1] Department of Earth and Planetary Science, School of Science, University of Tokyo, Hongo 7-3-1, Bunkyo, Tokyo 113-0033, Japan (trishit@eps.s.u-tokyo.ac.jp), [2]International Research School of Planetary Sciences, Università G. d'Annunzio, Viale Pindaro 42, 65127, Pescara, Italy, [3] Department of Ocean Floor Geoscience, Atmosphere and Ocean Research Institute, University of Tokyo, Kashiwanoha 5-1-5, Kashiwa, Chiba 277-8564, Japan, [4] Planetary Environmental and Astrobiological Research Laboratory, School of Atmospheric Sciences, Sun Yat-sen University, Zhuhai, China, [5] Department of Earth Sciences, Indian Institute of Technology Kanpur, Kanpur, UP 208016, India.

Introduction: We identified an unusually high number (>400) of boulder tracks from the on the southern inner wall and the central peak region of the Finsen crater located within the South Pole– Aitken (SPA) basin on the lunar far side (Fig. 1A and B). We assessed two main possibilities of triggers, 1) ground shaking excited by the recent impact crater formation events, and 2) moonquakes generated from recent fault reactivation (shallow quakes) associated with the lobate scarps identified inside and in the vicinity of Finsen.

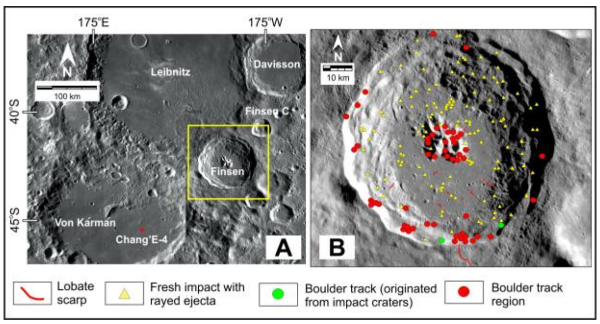

Fig. 1. (A) The Finsen crater is shown in the LRO–WAC mosaic regional context image. Both the Leibnitz and Von Kármán craters in the NW and the SW of Finsen preserves the Finsen ejecta. The red star indicates the location of Chang'E–4 landing site. **(B)** Distribution of boulder tracks, lobate scaps, and fresh impact craters within Finsen crater. Each marked mapped features are mentioned in the rectangle.

Boulder tracks on the lunar surface [1, 2, 3] bear the signature of dynamic geological activity. With the global availability of the high-resolution Lunar Reconnaissance Orbiter (LRO) Narrow–Angle Camera (NAC) images [4], it is now possible to explore the ground shaking triggering mechanisms responsible for the boulder falls with higher confidence. On the Moon, seismic ground shakings generated by shallow moonquakes have been correlated to the movements along young lobate scarps [2, 5, 6]. Apart from the shallow moonquakes, impact-induced ground shaking, and late-stage thermal contraction (resulting in lobate scarps) and its associated moonquakes [7, 8] also seem to play a salient role to dislodge the boulders from their initial places [2, 3, 9]. Meteorite impact-ejected boulder tracks are aligned radially around the impact sites and such impact-induced stresses also generate fracture networks in the surroundings for the boulders to form in the future [1]. Subsequently, thermal fatigue due to the diurnal temperature difference can enhance such fractures [10, 11]. However, the triggering mechanism of the boulder falls remains questionable due to the absence of any standout criteria to demarcate coseismic activities from the other ground-shaking agents.

The SPA basin has long been considered as an important landing site (first visited by the ongoing Chang'E–4 mission) due to its scientific significance including the mantle affinity [12] and volcanic activities [13]. Therefore, to aid in selecting a safe and prospective future landing site in the future with the potentials to understand mantle evolution and current geologic processes in the SPA basin, we carried out this research. Additionally, boulders are also key targets for future sample collection missions. If their origin is traced back using boulder tracks, they can reveal geologic information even from the inaccessible region of their origin.

Lobate Scarps and Seismicity: We have observed 19 segments of lobate scarps on the floor of Finsen and 2 segments adjacent to the rim on the southern crater wall (Fig. 1B). The minimum fault length (L = horizontal length of the fault) is 110 m and the maximum fault length is 8.176 km (mean 1.079 km). These lobate scarps trend NE–SW to NW–SE and had not been reported previously. The orientations of the lobate scarps are at a high angle to the predicted lunar fault orientation by Watters et al. (2015) [14], where the responsible stress originated due to the combination of recession stresses, diurnal tidal stresses at apogee, orbital recession, and isometric compression [6]. Therefore, other stresses might be responsible for the formation of the lobate scarps in the region but their reactivation could be favored by these combined modelled stresses.

We found that these lobate scarps could have generated moment magnitude (M_W) 3.56 to 7.17 moonquakes. Here, we estimate the moment magnitude considering the Finsen and the adjacent area are dominated by basaltic rocks of the SPA floor. However, these values are higher than the recorded moonquakes by the Apollo missions [6, 15]. Nevertheless, a M_W 6.36 quake was estimated by Watters et al. (2019) [6] considering a large number of lobate scarps.

Impact-induced seismicity: We used the UV–VIS [16] derived optical maturity map, to trace the fresh impact craters with bright ejecta. We found 134 such craters within 4176 km^2 of the crater floor with a maximum diameter of 202 m, and a mean diameter of 61.5 m. Calculating the equivalent seismic moment from individual impact events, following Teanby and Wookey (2011) [17], we estimated that the 202 m and 61.5 m diameter crater could have produced M_w 3.67 and 2.82 magnitude moonquake respectively. This moonquake should be enough to initiate dry granular flows from steep surfaces of the Moon. Moreover, the large shallow moonquakes observed by the Apollo seismometers are within a similar range.

Discussion on the potential triggers: From the critical point of view, the previously mentioned phenomena (shallow seismic shaking and impact-induced ground shaking) could individually or in combination can trigger boulder falls. Watters et al. (2019) [6] reevaluated the epicentral locations of the observed shallow moonquakes with the short 8-year timeframes and found the trace of one fault within 30 km from each moonquake epicenter. It should be mentioned that the location of the Finsen crater is in between the central and mid-ring of the SPA basin [18], and its (Finsen crater) central peak is positioned just above the boundary. This interpretation is consistent with the data extracted from the GRAIL (Gravity Recovery and Interior Laboratory) crustal thickness map (Fig. 2), and Bouguer gravity [19] maps. Furthermore, the NE-SW oriented lobate scarps coincide with the central ring curvature of the SPA basin. In general, such basin rings are associated with multiple inward dipping normal faults with steep slopes [20] and create a weak zone along the structural discontinuity. Thus, these NE-SW oriented lobate scarps could be related to the later reactivation and a smaller component of reverse motion along the pre-existing normal fault.

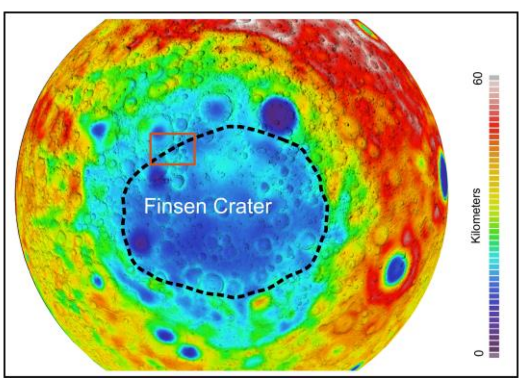

Fig. 2. GRAIL crustal thickness map (inferred from the Bouguer gravity map) of the SPA basin region (assuming the density of the crust is uniform), includes shaded relief of the surface features. The black dotted line indicates the boundary between the central and outer rings of the SPA basin. The locations of the Finsen crater is marked with the red rectangle.

On the other hand, impact craters are more evenly distributed. The highest seismic moment (M_W 3.67) these craters could have generated is comparable to the moonquake whose epicenter was at the Laue crater (M_W 4.1 [2]. Therefore, we cannot entirely abandon the possibility of the necessary ground shaking originating from the impacts.

Conclusion: Considering the distribution of the lobate scarps and the spatial distribution of the boulder tracks within the Finsen crater, our investigation revealed some parts of the SPA basin is tectonically active and has remained active in the recent past. The central and mid-ring boundary of the SPA basin, as a form of structural discontinuity zone, coincides with the orientations of the lobate scarps and the distribution of the boulders within the Finsen crater.

The estimated moonquakes (M_W=7.9) generated from the movements along the faults, are higher than the impact-induced moonquakes (M_W=3.67). Therefore, these shallow moonquakes with higher M_W are possibly the major triggers for the present-day boulder falls. Nevertheless, we cannot exclude the possibility of impact-induced ground-shaking responsible for the formation of at least some boulders in the area. The presently available dataset does not allow us to discriminate which factor is responsible for individual boulder falls. In the future, we recommend taking special attention for the human and landing missions around the structural discontinuity zones of the SPA basin, as these regions could be potentially more hazardous than the other parts of the basin.

Acknowledgments: TR and KK acknowledge JSPS KAKENHI Grant Number JP 18F18312.

References: [1] Bickel V.T. et al. (2020) *Nat. Commun., 11,* 2862. [2] Senthil Kumar P. et al. (2019) *GRL, 46,* 7972–7981. [3] Senthil Kumar P. et al. (2016) *JGR Planets, 121,* 147–179. [4] Robinson M.S. et al. (2010) *Space Sci. Rev.*, 150, 81–124. [5] van der Bogert C. H. et al. (2018) *Icarus, 306,* 225–242. [6] Watters T.R. et al. (2019) *Nat. Geosci. 12,* 411–417. [7] Banks M. E. et al. (2012) *JGR Planets, 117.* [8] Watters T. R. et al. (2010) *Science, 329,* 936–940. [9] Xiao Z. et al. (2013) *Earth Planet. Sci. Lett., 376,* 1–11. [10] Molaro J. L. et al. (2017) *Icarus, 294,* 247–261. [11] Ruesch O. et al. (2020) *Icarus, 336,* 113431. [12] Melosh H. J. et al. (2017) *Geology, 45,* 1063–1066. [13] Pasckert J. H. et al. (2018) *Icarus, 299,* 538–562. [14] Watters T. R. et al. (2015) *Geology, 43,* 851–854. [15] Shirley J. H. (1986) *Earth Planet. Sci. Lett. 76,* 241–253. [16] Lucey P. G. et al. (2000) *JGR Planets, 105,* 20377–20386. [17] Teanby N. A. and Wookey J. (2011) *Phys. Earth Planet. Inter., 186,* 70–80. [18] Garrick-Bethell L. and Zuber M. T. (2009) *Icarus, 204,* 399–408. [19] Zuber M. T. et al. (2013) *Science, 339,* 668–671. [20] Allemand P. and Thomas P. (1999) *JGR Planets, 104,* 16501–16514.